ELSEVIER

Cracks and re-entrant corners in functionally graded materials

Alberto Carpinteri *, Nicola Pugno

Department of Structural Engineering, Politecnico di Torino, Corso Duca degli Abruzzi 24, 10129 Torino, Italy

Abstract

Functionally graded materials (FGMs) are special composites in which the volume fractions of constituent materials vary gradually, giving continuously graded mechanical properties. The aim of this paper is the evaluation of the strength of structures composed by FGMs incorporating re-entrant corners – tending to the more common crack for vanishing corner angle. The end result is useful in engineering applications predicting the strength of the element corresponding to the unstable brittle crack propagation in such innovative materials. To show the general validity of the method, heterogeneous plates under tension and beam under bending containing re-entrant corners and by varying corner angle, depth and grading of the FGM are considered. Ad hoc performed numerical finite element simulations, by using the FRANC2D code, agree with the theoretical predictions.
© 2006 Elsevier Ltd. All rights reserved.

Keywords: Re-entrant corner; Crack; Functionally graded material; Fracture; Strength

1. Introduction

Non-homogeneous material systems with gradual variation in properties are collectively referred to as functionally graded materials or FGMs. The spatial variation of the elastic and physical properties of the material makes FGMs an attractive alternative to composite solids opening new possibilities for optimizing both material and component structures to achieve high performance and material efficiency. Gradual variation of material properties in FGMs, unlike abrupt changes encountered in discretely layered systems, is known to improve failure performance while preserving the intended thermal, tribological, and/or structural benefits of combining dissimilar materials. Consequently, the concept of using FGMs, for improving material performance has recently received considerable attention from the research community [1]. On the other hand, it also poses at the same time challenging mechanics problems including the understanding of damage and fracture behavior of such materials. The fracture behaviour of FGMs is an important design consideration. A crack in a FGM may exhibit complex behaviour [2,3]. Significant efforts on FGMs have been made in the study of cracks but the more general problem of a re-entrant corner [4] – tending to an edge crack for vanishing corner angle – has not been treated until now. This represents the aim of the present analysis.

---

* Corresponding author.
  E-mail addresses: alberto.carpinteri@polito.it (A. Carpinteri), nicola.pugno@polito.it (N. Pugno).

Nomenclature

E	Young's modulus
N	axial force
M	bending moment
A^*	elastic cross-section area
S^*	elastic static moment
I^*	elastic inertia moment
σ	applied stress
σ_{ij}	stress-field
σ_C	critical (failure) stress
σ_u	material strength
K_I	stress-intensity factor (Mode I)
K_{IC}	material fracture toughness (Mode I)
r, φ	polar co-ordinates
y	rectangular co-ordinate
α	power of the stress singularity
S_{ij}	function describing the angular profile of the stress-field
f	shape function for a crack
g	generalized shape function for a flat angle
b	structure height
a	defect length
γ	re-entrant corner angle
l	structure length
t	structure thickness
P	applied load
P_C	critical (failure) load
d_0	fracture quantum
s	brittleness number

Superscripts

*	generalized quantities for re-entrant-corners ($0 < \gamma < \pi$)
π	generalized quantities evaluated for a flat angle ($\gamma = \pi$)
^	generalized quantities for functionally graded materials (absence of superscripts denotes homogeneous cracked structures, $\gamma = 0$; if not differently specified)

Some of the early works on the fracture mechanics of FGMs include those by Atkinson and List [2], and Delale and Erdogan [3]. They show that the asymptotic crack tip stress field possesses the same square root singularity as that in homogeneous materials. It was later confirmed by Eischen [5] using eigenfunction asymptotic analysis. According to this result the asymptotic stress field near the crack tip in FGMs can be expressed as that in homogeneous materials. In particular, in [3] it has been studied analytically the behaviour of a crack in an infinite FGM plate with the elastic material constants varying in the direction parallel to the crack. This study indicates that Young's modulus has a significant effect on the stress field, but the effect of Poisson's ratio can be ignored. More recently Erdogan and co-workers [6] propose the multiplication of the conventional singular stress at a given point by the ratio of the Young's modulus evaluated at that point and at the crack tip. This hypothesis satisfies the equations of compatibility exactly, although – being limited in its own region of dominance – it obviously does not satisfy the conditions for equilibrium. In that paper [6] – summarizing recent advances in fracture mechanics of FGMs – theoretical results for cracks oriented along the elastic gradient and subjected to various loading conditions are also presented.

Extensive research on various aspects of fracture of isotropic FGMs has been conducted not only under mechanical loads, as previously discussed, but also under thermal loads [7–12]. Mixed-mode [4,13,14] crack problems have been investigated. Ozturk and Erdogan [13,14] used integral equations to investigate Mode I and mixed-mode crack problems in an infinite non-homogeneous orthotropic medium with a crack aligned with one of the material directions considering constant Poisson's ratio. Among the dynamic investigations on FGMs, transient stress-intensity factors for a Mode III crack lying in an elastic media with spatially varying elastic properties normal to crack surfaces has been studied analytically by Babaei and Lukasiewicz [15]. Experimental investigations into the fracture of FGMs are limited due to the high cost and elaborate facilities required for processing FGMs. Relatively fewer experimental and numerical investigations of the fracture behaviour of FGMs have been conducted. Among the few experimental mechanics investigations on FGMs, Parameswaran and Shukla [16] have shown experimentally that increasing toughness in the direction of crack growth reduces crack jump distance in discretely layered FGMs.

In spite of these efforts, the understanding of the fracture process at the vertex of a crack tip in FGMs is still limited and entirely absent for the more general re-entrant corner; fracture mechanics applied to sharp cracks has been broadly developed in the last three decades, even if only as a special case of the more general problem of re-entrant corners.

Since the pioneer paper [4] the problem of stress intensification at the vertex of re-entrant corners has not been sufficiently addressed if compared with its considerable practical importance also in homogeneous structure [17–27].

The investigation on stress intensification at the vertex of re-entrant corners carried out at CSIRO Australian Forest Production Laboratory, Division of Building Research is very notable. In [17] the size scale effects in structures with re-entrant corners due to the presence of a stress-singularity, noting that they occur only when the member sizes are sufficiently large, have been emphasized. Consequently, such scale effects may not appear in scaled-down laboratory testing. The work presented in [17] was continued in [18] extending conventional finite element procedures to non-zero angle notch problems. The author considered also the problem of crack initiation at corners of openings in walls and examined the effect of beam size on the sharp crack propagation in concrete [19]. In [20] the determination of realistic measures for the peak local stresses occurring at sharp re-entrant corners in plates under remote transverse loading has been considered. The authors took up the singular character of re-entrant corners and carried out experimental investigation on classical stress concentration. Then, the Reciprocal Work Contour Integral Method was used to obtain the stress singularity at the tip of corner configurations [21]. In this way, the numerical analysis of a lap joint with $\pi/2$ corner angles in mixed mode loading has been performed. In [22] the expression of the brittleness number to study the transition between brittle and stress collapses and the stress-intensity factor at the vertex of a re-entrant corner applying Buckingham's Theorem have been generalized. In the same paper a shape function for generalized stress-intensity factor, assuming a combination of LEFM and ultimate strength function, is defined. According to the last hypothesis and to the results of an experimental investigation, the values of stress-intensity factors varying the corner angle are reported.

More recently some authors [23] have obtained numerically, by Finite Element Method (FEM), the shape function for a re-entrant corner with particular angles $(0, \pi/2, 2\pi/3)$. In [24] the stress and strain fields at the vertex of a corner subjected to different boundary conditions, in plane problems of elasticity have been studied. In [25] the problem of evaluating linear elastic stress fields in the area of cracks and notches by Muskhelishvili's method based on complex functions has been consider. The stress-intensity factors of angular corners have been also calculated for various geometrical and loading conditions by numerical solutions of singular integral equations [26].

In [27] a relation between the stress-intensity factor for a corner and that for a crack, obtained from the Novozhilov's brittle fracture criterion [28], is presented. It is taken into account in [29]. The criterion [28] is based on the hypothesis that the fracture of solids is a discrete process. We note here that a powerful theory, namely Quantized Fracture Mechanics [30], the energy analog of the stress-based Novozhilov's approach, has been recently proposed and demonstrated to be valid also at the nanoscale. Based on this hypothesis the prediction of the failure load for a homogeneous structural member with a re-entrant corner has been recently obtained from a theoretical viewpoint [31,32]. Experiments agree with that predictions.

The theory herein developed represents the natural extension of the previous approach – dealing with re-entrant corners in homogeneous materials – for FGMs. The results are the predictions of stress-intensity factors, shape functions and strengths for FGMs composite structural elements with re-entrant corners. Numerical FEM simulations agree well with our theory.

2. Functionally graded materials

In the study of structures composed by linear elastic FGMs under axial load and bending moment (Figs. 1 and 2), we assume the conservation of the plane sections, as proposed in the study of multi-layered beam, see [33]. The result is that the stress is not linear (along y) and can be evaluated as

$$\sigma(y) = \frac{E(y)}{E_r}\left(\frac{N}{A^*} + \frac{M}{I^*}y\right) \tag{1}$$

where E_r is an arbitrary constant reference value of Young' modulus, N and M the axial load and the bending moment applied at the considered section and

$$A^* = \int_A \frac{E(y)}{E_r}\,\mathrm{d}A \tag{2}$$

is the *elastic* area, as well as

$$I^* = \int_A \frac{E(y)}{E_r}y^2\,\mathrm{d}A \tag{3}$$

represents the *elastic* moment of inertia.

The origin of the reference system, the *elastic* centroid, is defined from the following relationship:

$$S^* = \int_A \frac{E(y)}{E_r}y\,\mathrm{d}A = 0 \tag{4}$$

From these equations we can evaluate the stresses and predict the strength for uncracked heterogeneous members. The physical meaning of the *elastic* quantities is clear: they intrinsically take into account the stiffness of the structure, representing a generalization for the heterogeneous case of the homogeneous counterpart.
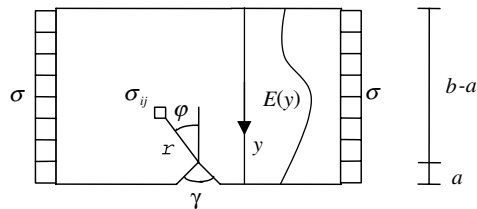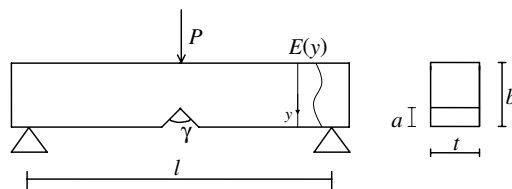

Fig. 1. Functionally graded plate in tension.

Fig. 2. Functionally graded beam under three-point bending.

3. FGM composite plate in tension

Considering a linear elastic homogeneous plate with a boundary crack (Fig. 1, with $\gamma = 0$), the symmetrical stress field around the tip of the crack can be written as

$$\sigma_{ij} = K_I r^{-1/2} S_{ij}(\varphi) \tag{5}$$

where K_I is the stress-intensity factor for the Mode I, r and φ are the polar co-ordinates represented in Fig. 1 and S_{ij} is a function describing the angular profile of the stress field.

For every structure it is possible to express the stress intensity factor as

$$K_I = \sigma b^{1/2} f(a/b) \tag{6}$$

where σ is the far field stress, b is a characteristic size of the structure, a is the crack length and f is a shape function depending on the geometry of structure and on the ratio a/b. The stress of failure σ_C is achieved when K_I is equal to its critical value K_{IC}

$$K_{IC} = \sigma_C b^{1/2} f(a/b) \tag{7}$$

Eischen [5] studied the stress and displacement fields around the crack tip in a non-homogeneous structure whose elastic moduli were specified by continuous and generally differentiable functions. Its results show that the correlation between the asymptotic stress singular field at the crack tip $\hat{\sigma}_{ij}$ and the corresponding stress intensity factor $\widehat{K}_I$ for the non-homogeneous structure is of the same form as that for the homogeneous structure of Eq. (5)

$$\hat{\sigma}_{ij} = \widehat{K}_I r^{-1/2} S_{ij}(\varphi) \tag{8}$$

The superscript "$\hat{}$" here distinguishes the heterogeneous case from the homogeneous one.

The presented equations can be generalized to the case of re-entrant corner with angle γ (Fig. 1).

When both the notch surfaces are free, the symmetrical stress field at the notch tip for the homogeneous structure is [22]

$$\sigma_{ij}^* = K_I^*(\gamma) r^{-\alpha(\gamma)} S_{ij}^{(\gamma)}(\varphi) \tag{9}$$

where the power α of the stress singularity is provided by the eigen-equation

$$(1 - \alpha) \sin(2\pi - \gamma) = \sin[(1 - \alpha)(2\pi - \gamma)] \tag{10}$$

and ranges between 1/2 (when $\gamma = 0$) and zero (when $\gamma = \pi$). Note that for Mode II crack propagation the same eigen-equation holds if one of the two sides is multiplied by the factor -1. Accordingly, three regions can be deduced: (i) $0 < \gamma < 0.51\pi$, in which both the crack propagation modes I and II present stress-singularities, (ii) $0.51\pi < \gamma < \pi$ where only the mode I stress-field is singular and (iii) $\pi < \gamma < 2\pi$ for which both the stress-fields are not singular.

The superscript "*" here describes generalized quantities from the classical case of a crack to re-entrant corners. Analogously, for FGMs is

$$\hat{\sigma}_{ij}^* = \widehat{K}_I^*(\gamma) r^{-\alpha(\gamma)} S_{ij}^{(\gamma)}(\varphi) \tag{11}$$

If Buckingham's Theorem for physical similitude and scale modelling is applied and stress and linear size are assumed as fundamental quantities [22], an equation analogous to Eq. (6) has to be written as

$$\widehat{K}_I^*(\gamma) = \hat{\sigma}^* b^{\alpha(\gamma)} \hat{f}^*(\gamma, E(y), a/b); \quad [\widehat{K}_I^*] = [F][L]^{\alpha-2} \tag{12}$$

in which appears a generalized shape function dependent on re-entrant corner angle and Young's modulus grading. When the heterogeneous structure becomes homogeneous (symbols without $\hat{}$, $E(y) = \text{const}$) and the angle γ vanishes, Eq. (12) must coincide with Eq. (6), whereas when $\gamma = \pi$ the stress-singularity disappears and the generalized stress intensity factor $\widehat{K}_I^*$ assumes the physical dimensions of stress and becomes proportional to the nominal stress. The stress of failure $\hat{\sigma}_C$ is achieved when $\widehat{K}_I^*$ is equal to its critical value $\widehat{K}_{IC}^*$

$$\widehat{K}_{IC}^*(\gamma) = \hat{\sigma}_C^* b^{\alpha(\gamma)} \hat{f}^*(\gamma, E(y), a/b) \tag{13}$$

Three of four limit cases of Eq. (13) – concerning crack and flat angle in homogeneous structures and flat angles in heterogeneous structures – are actually known. If the angle is close to zero in an homogeneous structure, the corner becomes a crack and Eq. (13) becomes Eq. (7), where f is the known corresponding shape function, e.g. ($a/b < 0.6$) [31]

$$f\left(\frac{a}{b}\right) = 2\left(\frac{a}{b}\right)^{1/2} - 0.4\left(\frac{a}{b}\right)^{3/2} + 18.7\left(\frac{a}{b}\right)^{5/2} - 38.5\left(\frac{a}{b}\right)^{7/2} + 53.9\left(\frac{a}{b}\right)^{9/2} \tag{14}$$

In the case of angle close to π in heterogeneous structure, Eq. (13) becomes

$$\widehat{K}_{\mathrm{IC}}^*(\gamma = \pi) = \hat{\sigma}_u = \hat{\sigma}_{\mathrm{C}}^\pi \hat{f}^*(\gamma = \pi, E(y), a/b) \equiv \hat{\sigma}_{\mathrm{C}}^\pi \hat{g}(E(y), a/b) \tag{15}$$

where $\hat{\sigma}_u$ is the strength of the material at the crack tip and the function $\hat{g}$ takes into account the reduction of the resisting cross-section. It can be obtained by integration over the ligament area, as suggested by Eq. (2)

$$\hat{g}(E(y), a/b) = \frac{\int_A E(y)\,\mathrm{d}A}{\int_{A_{\mathrm{lig}}} E(y)\,\mathrm{d}A} \tag{16}$$

For flat angle in homogeneous structure it becomes

$$g\left(\frac{a}{b}\right) = \hat{g}(E(y) = \mathrm{const}, a/b) = \frac{1}{1 - a/b} \tag{17}$$

The other limit case of Eq. (13), concerning a crack in FGM, as well as $\hat{f}(E(y), a/b)$ and the general form of $\hat{f}^*(\gamma, E(y), a/b)$, is actually unknown.

4. FGM composite beam under three-point bending

The same considerations can be done for different geometries, e.g. a beam composed by FGMs under three-point bending. A three-point bending FGM composite specimen with a re-entrant corner is now considered (Fig. 2). The stress-intensity factor can be expressed as [22]

$$\widehat{K}_{\mathrm{I}}^*(\gamma) = \frac{\widehat{P}^* l}{t b^{2-\alpha(\gamma)}} \hat{f}^*(\gamma, E(y), a/b) \tag{18}$$

that, in critical condition, becomes

$$\widehat{K}_{\mathrm{IC}}^*(\gamma) = \frac{\widehat{P}_{\mathrm{C}}^* l}{t b^{2-\alpha(\gamma)}} \hat{f}^*(\gamma, E(y), a/b) \tag{19}$$

For a crack in an homogeneous beam Eq. (19) assumes the well-known following form:

$$K_{\mathrm{IC}} = \frac{P_{\mathrm{C}} l}{t b^{3/2}} f(a/b) \tag{20}$$

where the function f is well-known and can be expressed as follows ($a/b < 0.6$) [30]:

$$f\left(\frac{a}{b}\right) = 2.9\left(\frac{a}{b}\right)^{1/2} - 4.6\left(\frac{a}{b}\right)^{3/2} + 21.8\left(\frac{a}{b}\right)^{5/2} - 37.6\left(\frac{a}{b}\right)^{7/2} + 38.7\left(\frac{a}{b}\right)^{9/2} \tag{21}$$

If we consider a flat angle

$$\widehat{K}_{\mathrm{IC}}^*(\gamma = \pi) = \hat{\sigma}_u = \frac{\widehat{P}_{\mathrm{C}}^\pi l}{t b^2} \hat{g}(E(y), a/b) \tag{22}$$

where the function $\hat{g}(E(y), a/b)$ describes the reduction of the resisting cross-section and can be evaluated by integration over the ligament area, as suggested by Eq. (3)

$$\hat{g}(E(y), a/b) = \frac{\widehat{E} t b^2 \hat{y}/4}{\int_{A_{\mathrm{lig}}} E(y) y^2\,\mathrm{d}A} \tag{23}$$

where $\widehat{E}$ is the Young's modulus evaluated at the crack tip, and $\hat{y}$ being the co-ordinate of the crack tip with respect to the reference system defined – as suggested by Eq. (4) – by $\int_{A_{\text{lig}}} E(y)y\,\mathrm{d}A = 0$. For an homogeneous structure it becomes

$$g\left(\frac{a}{b}\right) = \hat{g}(E(y) = \text{const}, a/b) = \frac{3/2}{(1 - a/b)^2} \tag{24}$$

The other limit case of Eq. (19), concerning a crack in FGM is, as well as $\hat{f}(E(y), a/b)$ and the general form of $\hat{f}^*(\gamma, E(y), a/b)$, actually unknown.

5. Stress intensity factor

In [27] a relation between the stress-intensity factor for a re-entrant corner and that for a crack is obtained from the brittle fracture criterion presented in [28].

The brittle fracture criterion [28] should be written in the following integral form:

$$\int_0^{d_0} \hat{\sigma}^*(y)\,\mathrm{d}y \geqslant \hat{\sigma}_u d_0 \tag{25}$$

where $\hat{\sigma}_u$ is a strength characteristic value for the material without defects and d_0 is a finite length [28,30,31]. According to the Eischen solution [5], substituting the stress field around the vertex of the corner in FGMs – given by Eq. (11) – into Eq. (25), we can rewrite the condition for brittle propagation as

$$\widehat{K}_{\mathrm{I}}^*(\gamma) \geqslant [1 - \alpha(\gamma)](2\pi d_0)^{\alpha(\gamma)}\hat{\sigma}_u \tag{26}$$

where the right part of the inequality must represent the critical value of the stress-intensity factor

$$\widehat{K}_{\mathrm{IC}}^*(\gamma) = [1 - \alpha(\gamma)](2\pi d_0)^{\alpha(\gamma)}\hat{\sigma}_u \tag{27}$$

Evaluating Eq. (27) for a crack we obtain d_0 (it is interesting to emphasize that d_0 coincides with Irwin's estimate of the plastic zone diameter)

$$d_0 = \frac{2}{\pi}\frac{\widehat{K}_{\mathrm{IC}}^2}{\hat{\sigma}_u^2} \tag{28}$$

Thus rather than a constant it is expected to vary with the structural size as the nominal strength and fracture toughness of the material [34].

Substituting d_0 into Eq. (27) yields

$$\widehat{K}_{\mathrm{IC}}^*(\gamma) = (1 - \alpha(\gamma))\hat{\sigma}_u\left(\frac{2\widehat{K}_{\mathrm{IC}}}{\hat{\sigma}_u}\right)^{2\alpha(\gamma)} \tag{29}$$

Erdogan [6] proposes the following extension to the Eischen solution [5] of Eq. (8):

$$\hat{\sigma}_{ij} = \frac{E(r, \varphi)}{E(0, \varphi)}\widehat{K}_{\mathrm{I}}r^{-1/2}S_{ij}(\varphi) \tag{30}$$

that, in any case, for small r coincides with the Eischen's solution [5] of Eq. (8). Eq. (30) can be rewritten for a re-entrant corner as follows:

$$\hat{\sigma}_{ij}^* = \frac{E(r, \varphi)}{E(0, \varphi)}\widehat{K}_{\mathrm{I}}^*(\gamma)r^{-\alpha(\gamma)}S_{ij}^{(\gamma)}(\varphi) \tag{31}$$

Considering Eq. (31) instead of Eq. (11) into Eq. (25) gives a better estimation for the stress-intensity factor in FGMs. On the other hand, it implies only very weak corrections, with exception for the cases of very high Young's modulus gradients.

6. Shape function

The embrittlement of the structural response produced by the decrease in fracture toughness and/or by the increase in strength σ_u and/or in the size b, can be described in a unitary and synthetic manner via the variation in the dimensionless numbers [31] for FGMs

$$\hat{s}^*(\gamma) = \frac{\widehat{K}^*_{\mathrm{IC}}(\gamma)}{\hat{\sigma}_u b^{\alpha(\gamma)}} \tag{32}$$

Larger the number $\hat{s}^*(\gamma)$, larger the structure ductility. If it is over than a characteristic number $\hat{s}^*_0(\gamma)$ the stress collapse ($\hat{\sigma}^* = \hat{\sigma}_u$) precedes the generalized brittle collapse ($\widehat{K}^*_{\mathrm{I}}(\gamma) = \widehat{K}^*_{\mathrm{IC}}(\gamma)$) for any relative corner depth a/b. Eq. (32) shows that the brittleness and the ductility are structure-characteristics more than material-characteristics: increasing the size b of the structure its embrittlement increases. Taking into account Eq. (29), relation (32) may be reformulated in a generalized form:

$$\hat{s}^*(\gamma) = (1 - \alpha(\gamma))(2\hat{s})^{2\alpha(\gamma)} \tag{33}$$

In the opposite cases of crack or corner angle close to π (flat angle) we respectively obtain

$$\hat{s} = \hat{s}^*(\gamma = 0) = \frac{\widehat{K}_{\mathrm{IC}}}{\hat{\sigma}_u \sqrt{b}} \tag{34a}$$

$$\hat{s}^*(\gamma = \pi) = 1 \tag{34b}$$

The last trivial equation has the meaning that for an uncracked structure the generalized brittle and the stress collapses are coincident.

Considering a three point bending specimen and substituting Eq. (32) into Eq. (19) we obtain the dimensionless failure load as a function of the generalized brittleness number and of the shape function

$$\frac{\widehat{P}^*_{\mathrm{C}} l}{tb^2 \hat{\sigma}_u} = \frac{\hat{s}^*(\gamma)}{\hat{f}^*(\gamma, E(y), a/b)} \tag{35}$$

This kind of failure, when $\widehat{K}^*_{\mathrm{I}}(\gamma) = \widehat{K}^*_{\mathrm{IC}}(\gamma)$, is always intermediate between brittle $[\widehat{K}_{\mathrm{I}} = \widehat{K}_{\mathrm{IC}}]$ and stress $[\hat{\sigma}^* = \hat{\sigma}_u]$ collapses. We here refer to the "stress collapse" for stress-controlled failure, i.e., when the maximum stress reaches the material strength, in contrast to the brittle collapse arising when the stress-intensity factor equals the material fracture toughness. We do not consider here plastic reserves, assuming for each point of the heterogeneous structure an isotropic linear elastic law.

Eq. (35) can be evaluated for a crack, as

$$\frac{\widehat{P}_{\mathrm{C}} l}{tb^2 \hat{\sigma}_u} = \frac{\hat{s}}{\hat{f}(E(y), a/b)} \tag{36}$$

and for a flat angle

$$\frac{\widehat{P}^\pi_{\mathrm{C}} l}{tb^2 \hat{\sigma}_u} = \frac{1}{\hat{g}(E(y), a/b)} \tag{37}$$

For a structural element with a crack of a given relative depth, the transition between brittle and stress collapse [22,31] arises when the failure loads (36) and (37) are equal for

$$\hat{s}_0 = \frac{\hat{f}(E(y), a/b)}{\hat{g}(E(y), a/b)} \tag{38}$$

If the angle is different from zero, the crack becomes a re-entrant corner and the transition arises when the failure loads (35) and (37) are equal for

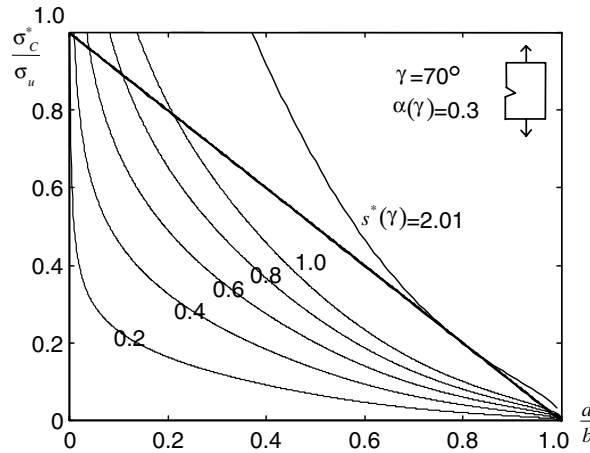$$\hat{s}^*_0(\gamma) = \frac{\hat{f}^*(\gamma, E(y), a/b)}{\hat{g}(E(y), a/b)} \tag{39}$$

Fig. 3. Competition between brittle (thin lines) and stress (thicker and straight line) collapses, in the case of homogeneous plate in tension with edge corner ($\gamma = 70°$). Stress-controlled failure preceding brittle collapse describes a flaw-tolerance for the heterogeneous V-notched structure.

The competition between the two kinds of collapses (35) and (37) is shown in the diagrams of Fig. 3 for the case of homogeneous structures. The value of the brittleness number for which the corresponding generalized fracture curve (35) is tangential to the curve of stress collapse (38) represents its characteristic value; for higher values of $\hat{s}^*$ the stress collapse precedes the generalized brittle collapse for any relative corner depth and thus a "flaw-tolerance" behaviour is observed.

Substituting Eqs. (38) and (39) into Eq. (33) we obtain the generalized shape function for the re-entrant corner

$$\hat{f}^*(\gamma, E(y), a/b) = (1 - \alpha(\gamma))\hat{g}(E(y), a/b)\left(2\frac{\hat{f}(E(y), a/b)}{\hat{g}(E(y), a/b)}\right)^{2\alpha(\gamma)} \tag{40}$$

Exactly the same result can be found for plates in tension. It is to underline that, at the moment, function $\hat{f}(E(y), a/b)$ is our last unknown. This function, for a specified variation of the Young's modulus $E(y)$, can be easily obtained numerically, as done by function f for homogeneous structures. An analytical solution for this shape function will be proposed in the next section.

7. Strength

The result of Eq. (40) is important permitting, via Eqs. (29) and (13) or (19), to obtain the strength for a structure composed by FGMs with a re-entrant corner.

The stress intensity-factor (for a crack) and the ultimate tensile strength of the material of the element in object, can be respectively obtained as functions of the failure loads in the cases of angle equal to zero and flat angle. Substituting the generalized stress-intensity factor (29) and the shape function (40) into Eq. (13) or (19) we can obtain in a very synthetic form the failure load for a FGM composite member with a re-entrant corner

$$\frac{\widehat{P}_C^*}{\widehat{P}_C^\pi} = \left(\frac{\widehat{P}_C}{\widehat{P}_C^\pi}\right)^{2\alpha(\gamma)} \tag{41}$$

where, for a plate in tension $\widehat{P} \equiv \hat{\sigma}$. It is to underline that, at the moment, $\hat{f}$ and consequently $\widehat{P}_C$ are unknowns. Eq. (41) is formally identical to that derived for homogeneous structures [31].

To have an analytical form for $\hat{f}(E(y), a/b)$, we can start noting that the ratio $\frac{\widehat{P}_C^*}{P_C^*}$ is, as a first approximation, independent from the corner angle. In particular

$$\frac{\widehat{P}_{\mathrm{C}}^*}{P_{\mathrm{C}}^*} \approx \frac{\widehat{P}_{\mathrm{C}}^\pi}{P_{\mathrm{C}}^\pi} \tag{42a}$$

or equivalently

$$R = \frac{\widehat{P}_{\mathrm{C}}^*(E(y), \gamma, a/b) \cdot P_{\mathrm{C}}^\pi(a/b)}{P_{\mathrm{C}}^*(\gamma, a/b) \cdot \widehat{P}_{\mathrm{C}}^\pi(E(y), a/b)} \approx 1 \quad \forall E(y), \gamma, a/b \tag{42b}$$

Eq. (42b) is satisfied by the known limit cases – crack in homogeneous structure and flat angle in heterogeneous/homogeneous structures – and it appears verified for the other cases (crack and re-entrant corners in heterogeneous structure).

In order to perform an assessment of the presented theoretical formulation for FGMs, the parameter R of Eq. (42b) which represents a hypothesis of mechanical similarity was computed according to a numerical procedure based on generalized isoparametric finite elements by Lim and Lee [35]. The public domain FEM code FRANC2D (FRacture ANanlysis Code 2D) (developed by Wawrzynek and Ingraffea [36]) is used as a basic framework for this parametric study. Assuming a two-layer three-point bending beam, the simulations have been performed by varying the relative depth and the angle of the re-entrant corner as well as the grading of the FGM. In particular a two-layered element is analysed by varying the thickness of the two layers and the ratio of the Young's moduli. Stress-intensity factors are worked out by applying a displacement correlation technique, as also proposed in [35]. In these analyses, special attention is devoted to the proper representation of the singular stress field near the singular points. Therefore, in the case of re-entrant corners, as well as for a crack perpendicular to a bi-material interface, the order of the stress-singularity is preliminary worked out by performing an asymptotic analysis. Then, by varying the placement of the mid-side node between quarter-point and the mid-point position, the given order of the stress-singularity is modeled. The displacement correlation technique is also generalized for treating these particular situations. More details about the numerical method can be found in [37]. As theoretically predicted, parameter R appears very close to the unity [37], showing that the hypotheses made for the derivation of the theoretical formulation are basically correct. The larger but still contained (of the order of 10%) discrepancies with respect to the FEM simulations are found for corner tips close to interface planes, for which a stronger stress singularity is expected.

Thus the numerical analysis clearly confirm that Eq. (42b) is valid and consequently, we have – see Eq. (13) or (19)

$$\frac{\hat{f}^*(\gamma, E(y), a/b)}{f^*(\gamma, a/b)} = \frac{\hat{g}(E(y), a/b)}{g(a/b)} \left(\frac{\sigma_u \widehat{K}_{\mathrm{IC}}}{\hat{\sigma}_u K_{\mathrm{IC}}} \right)^{2\alpha(\gamma)} \tag{43}$$

Eq. (43) gives an identity for the limit case of flat angle. On the other hand, considering the limit case of a crack, we obtain the function $\hat{f}(E(y), a/b)$

$$\hat{f}(E(y), a/b) = \frac{\sigma_u \widehat{K}_{\mathrm{IC}}}{\hat{\sigma}_u K_{\mathrm{IC}}} \frac{\hat{g}(E(y), a/b)}{g(a/b)} f(a/b) \tag{44}$$

and by Eq. (40), the shape function for a re-entrant corner in FGM composite structures can be determined. In addition, from Eq. (42) derives

$$\frac{\widehat{P}_{\mathrm{C}}^*}{P_{\mathrm{C}}^*} = \frac{\hat{\sigma}_u}{\sigma_u} \frac{g(a/b)}{\hat{g}(E(y), a/b)} \tag{45}$$

and as limit cases

$$\widehat{P}_{\mathrm{C}} = P_{\mathrm{C}} \frac{\hat{\sigma}_u}{\sigma_u} \frac{g(a/b)}{\hat{g}(E(y), a/b)} \tag{46a}$$

$$\widehat{P}_{\mathrm{C}}^\pi = P_{\mathrm{C}}^\pi \frac{\hat{\sigma}_u}{\sigma_u} \frac{g(a/b)}{\hat{g}(E(y), a/b)} \tag{46b}$$

From Eq. (41) we can evaluate $\widehat{P}_C^*$ starting from the known values of $\widehat{P}_C$ and $\widehat{P}_C^\pi$ of Eqs. (46) simply evaluating $\hat{g}$ by Eq. (16) for a plate in tension or (23) for a beam under bending moment. The stress-intensity factor is given by Eq. (29), as well as the shape function is given by Eq. (40) in which we have to substitute Eq. (44). As a consequence – for a specified grading – we can easily solve the problem simply evaluating $\hat{g}$.

Note that the analysis assumes a notch tip with vanishing radius. On the other hand a simple correction to take into account the presence of a blunting can be derived according to Quantized Fracture Mechanics, see [30].

These theoretical results are very useful allowing to predict in a very simple manner the failure load for a structure composed by FGMs having re-entrant corners. The theory is applicable, as shown by the two examples of plates and beams, to different schemes and also with re-entrant corners not subjected only to Mode I: the generalization (29), as well as the extension of the Eischen result of Eq. (11) are also true for Modes II and III, considering the ultimate shearing stress and the stress-intensity factor for the corresponding Mode.

Introducing a characteristic maximum value $b_{\max}$ of the structure, from the generalized brittleness number (32), we can rewrite Eq. (13) emphasizing the attenuation of the size effects on the failure load when increasing the angle of the corner

$$\ln\frac{\hat{\sigma}_C^*}{\hat{\sigma}_u} = \ln\frac{\hat{s}^*(b_{\max})}{\hat{f}^*(\gamma, E(y), a/b)} - \alpha(\gamma)\ln\frac{b}{b_{\max}} \tag{47}$$

It shows that for $\alpha \neq 0$, the failure load decreases with size b. For an uncracked structure ($\alpha = 0$) the size effects vanish.

8. Simplified useful formulas

The formulas here deduced can be simplified noting that $(1 - \alpha(\gamma))2^{2\alpha(\gamma)} \approx 1$ for each value of γ (maximum error lower than 6% – see [31]) and $\frac{\sigma_u \widehat{K}_{IC}}{\hat{\sigma}_u K_{IC}} \approx 1$ (invariable finite length d_0). The generalized stress-intensity factor, can be simply obtained from the values of the strength $\hat{\sigma}_u$ and fracture toughness $\widehat{K}_{IC}$ of the material at the tip of the re-entrant corner and from the corresponding power of the singularity α (from Eq. (10))

$$\text{Stress-intensity factor:} \quad \widehat{K}_{IC}^* \approx \hat{\sigma}_u \left(\frac{\widehat{K}_{IC}}{\hat{\sigma}_u}\right)^{2\alpha} \tag{48}$$

The generalized shape functions can be obtained from the well-known values of f, g (Eqs. (14) and (17) for the plate, or (21) and (24) for the beam) as

$$\text{Shape function:} \quad \hat{f}^* \approx \hat{g}\left(\frac{f}{g}\right)^{2\alpha} \tag{49a}$$

where

$$\text{Plate in tension:} \quad \hat{g} = \frac{\int_A E(y)\,dA}{\int_{A_{\text{lig}}} E(y)\,dA}; \tag{49b}$$

$$\text{Beam under three point bending:} \quad \hat{g} = \frac{\widehat{E}tb^2\hat{y}/4}{\int_{A_{\text{lig}}} E(y)y^2\,dA}, \quad \text{Reference system:} \quad \int_{A_{\text{lig}}} E(y)y\,dA = 0 \tag{49c}$$

Finally, the strengths for FGM composite elements with re-entrant corners can obtained as

$$\text{Strength, plate in tension:} \quad \hat{\sigma}_C^* = \frac{\widehat{K}_{IC}^*}{b^\alpha \hat{f}^*}, \tag{50a}$$

$$\text{Strength, three-point bending beam:} \quad \widehat{P}_C^* = \frac{\widehat{K}_{IC}^* tb^{2-\alpha}}{l\hat{f}^*} \tag{50b}$$

Even if the theory is quite complex, the results are simple. An example of application is given in the next section. Thus, the proposed analytical approach could represent a key step towards an optimal design of FGM composite structures against crack propagation.

9. An example of application

The developed theory shows that to predict the strength of FGM structures containing re-entrant corners, we have to obtain the function $\hat{g}(E(y), a/b)$ for the specified grading. In this Section, an example is reported. We assume a Young's modulus (as well as the other material properties) linearly variable between two given values, E_1 (at the fiber where the re-entrant corner is placed) and E^1 (at the other external fiber). According to the formula reported in Section 8, for a plate in tension

$$\int_A E(y)\,\mathrm{d}A = \frac{tb}{2}(E_1 + E^1) \tag{51a}$$

$$\int_{A_{\mathrm{lig}}} E(y)\,\mathrm{d}A = \frac{t(b-a)}{2}(\widehat{E} + E^1) \tag{51b}$$

so that

$$\hat{g}(E(y), a/b) = \frac{\int_A E(y)\,\mathrm{d}A}{\int_{A_{\mathrm{lig}}} E(y)\,\mathrm{d}A} = \frac{E_1 + E^1}{\widehat{E} + E^1}\frac{1}{1 - a/b} = k_1 g\!\left(\frac{a}{b}\right) \tag{52}$$

On the other hand, for three-point bending

$$\hat{y} = \frac{\widehat{E} + 2E^1}{3(\widehat{E} + E^1)}(b - a) = \hat{k}(b - a) \tag{53}$$

$$\int_{A_{\mathrm{lig}}} E(y)y^2\,\mathrm{d}A = \left\{[1 + 6\hat{k}^2 - 4\hat{k}] + \frac{E^1}{\widehat{E}}[3 + 6\hat{k}^2 - 8\hat{k}]\right\}\widehat{E}\,\frac{t(b-a)^3}{12} = \hat{k}_2\widehat{E}\,\frac{t(b-a)^3}{12} \tag{54}$$

so that

$$\hat{g}(E(y), a/b) = \frac{\widehat{E}tb^2\hat{y}/4}{\int_{A_{\mathrm{lig}}} E(y)y^2\,\mathrm{d}A} = \frac{2\hat{k}}{\hat{k}_2}\frac{3/2}{(1 - a/b)^2} = k_2 g\!\left(\frac{a}{b}\right) \tag{55}$$

It is important to note that the value of the Young's modulus $\widehat{E}$ at the crack tip is it-self a function of the ratio a/b, i.e., $\widehat{E} = (E^1 - E_1)\frac{a}{b} + E_1$. Introducing this law in Eq. (52) or (55), from Eqs. (48), (49a) and (50) the strengths of the structure can be quantified.

10. Concluding remarks

The results of the paper are simple analytical laws to evaluate the strength of structures composed by FGMs incorporating re-entrant corners – tending to the more common crack for vanishing corner angle. The end findings are useful in engineering applications predicting the strength of the element corresponding to the unstable brittle crack propagation in such innovative materials. To show the general validity of the method, heterogeneous plates under tension and beam under bending, containing re-entrant corners, are considered. Propagations in different crack Mode conditions can be also treated. Ad hoc performed numerical FEM simulations, by varying corner angle, depth as well as grading of the FGM and by using the FRANC2D code, agree with the theoretical predictions.

Acknowledgements

References

[1] Special issue on fracture of functionally graded materials. Paulino GH (Guest editor), Engng Fract Mech 2002;69:1519–809.
[2] Atkinson C, List RD. Steady state crack propagation into media with spatially varying elastic properties. Int J Engng Sci 1978; 16:717–30.
[3] Delale F, Erdogan F. The crack problem for a non-homogeneous plane. J Appl Mech 1983;50:609–14.
[4] Williams ML. Stress singularities resulting from various boundary conditions in angular corners of plates in extension. J Appl Mech 1952;19:526–8.
[5] Eischen JW. Fracture of non-homogeneous materials. Int J Fract 1987;34:3–22.
[6] Erdogan F. Fracture mechanics of functionally graded materials. Compos Engng 1995;7:753–70.
[7] Jin ZH, Noda N. An internal crack parallel to the boundary of a non-homogeneous half plane under thermal loading. Int J Engng Sci 1993;31:793–806.
[8] Erdogan F, Wu BH. Crack problems in FGM layers under thermal stresses. J Therm Stresses 1996;19:237–65.
[9] Jin ZH, Batra RC. Stress intensity relaxation at the tip of an edge crack in a functionally graded material subjected to a thermal shock. J Therm Stresses 1996;19:317–39.
[10] Wang BL, Han JC, Du SY. Crack problems for functionally graded materials under transient thermal loading. J Therm Stresses 2000; 23:143–68.
[11] Jin ZH, Paulino GH. Transient thermal stress analysis of an edge crack in a functionally graded material. Int J Fract 2001;107:73–98.
[12] Wang BL, Noda N. Thermally induced fracture of a smart functionally graded composite structure. Theor Appl Fract Mech 2001; 35:93–109.
[13] Ozturk M, Erdogan F. Mode I crack problem in an inhomogeneous orthotropic medium. Int J Engng Sci 1997;35:869–83.
[14] Ozturk M, Erdogan F. The mixed mode crack problem in an inhomogeneous orthotropic medium. Int J Fract 1999;98:243–61.
[15] Babaei R, Lukasiewicz SA. Dynamic response of a crack in a functionally graded material between two dissimilar half-planes under anti-plane shear impact load. Engng Fract Mech 1998;60:479–87.
[16] Parameswaran V, Shukla A. Dynamic fracture of a functionally gradient material having discrete property variation. J Mater Sci 1998;33:3303–11.
[17] Leicester RH. Effect of size on the strength of structures. CSIRO Div Building Res 1973;71.
[18] Walsh PF. Linear fracture mechanics solutions for zero and right angle notches. CSIRO Div Building Res 1974;2.
[19] Walsh PF. Crack initiation in plain concrete. Mag Concrete Res 1976;28:37–41.
[20] Sinclair GB, Kondo M. On the stress concentration at sharp re-entrant corners in plates. Int J Mech Sci 1984;26:477–87.
[21] Carpenter WC. Mode I and Mode II stress intensities for plates with cracks of finite opening. Int J Fract 1984;26:201–14.
[22] Carpinteri A. Stress-singularity and generalized fracture toughness at the vertex of re-entrant corners. Engng Fract Mech 1987;26:143–55.
[23] Dunn ML, Suwito W, Cunningham S. Fracture initiation at sharp notches: correlation using critical stress intensities. Int J Solids Struct 1997;34:3873–83.
[24] Seweryn A, Molsky K. Elastic stress singularities and corresponding generalized stress intensity factors for angular corners under various boundary conditions. Engng Fract Mech 1996;55:529–56.
[25] Lazzarin P, Tovo R. A unified approach to the evaluation of linear elastic stress fields in the neighbohrood of cracks and notches. Int J Fract 1996;78:3–19.
[26] Noda NA, Oda K, Inoue T. Analysis of newly-defined stress intensity factors for angular corners using singular integral equations of the body force method. Int J Fract 1997;76:243–61.
[27] Seweryn A. Brittle fracture criterion for structures with sharp notches. Engng Fract Mech 1994;47:673–81.
[28] Novozhilov V. On a necessary and sufficient criterion for brittle strength. Prik Mat Mek 1969;33:212–22.
[29] Grenestedt JL, Hallstrom S, Kuttenkeuler J. On cracks emanating from wedges in expanded PVC foam. Engng Fract Mech 1996;54: 445–56.
[30] Pugno N, Ruoff R. Quantized fracture mechanics. Philos Mag 2004;84/27:2829–45.
[31] Carpinteri A., Pugno N. Structural elements with re-entrant corners. In: Proc XV Italian conf on frac, 3–5 May 2000, Bari, Italy; 2000. p. 391–8.
[32] Carpinteri A, Pugno N. Fracture instability and limit strength condition in structures with re-entrant corners. Engng Fract Mech 2005;72:1254–67.
[33] Carpinteri A. Structural mechanics: a unified approach, E&FN Spon; 1997.
[34] Carpinteri A, Pugno N. Are the scaling laws on strength of solids related to mechanics or to geometry? Nature Mater 2005(June): 421–3.
[35] Lim W, Lee C. Evaluation of stress intensity factors for a crack normal to bimaterial interface using isoparametric finite elements. Engng Fract Mech 1995;52:65–70.
[36] Wawrzynek PA, Ingraffea AR. Discrete modeling of crack propagation: theoretical aspects and implementation issues in two and three dimensions. Report 91-5, School of Civil and Environmental Engineering, Cornell University; 1991.
[37] Carpinteri A, Paggi M, Pugno N. Cracks and re-entrant corners in multi-layered elements. Int J Solid Struct 2006;43:627–41.